Int J CARS (2013) 8 (Suppl 1):S253–S257
DOI 10.1007/s11548-013-0877-8

Evaluation of the accuracy of three dimensional printed mandibular models generated from cone beam computed tomography data

N. Issa[1], N. Salah[1], H. Omar[1]
[1]Cairo University, Oral Radiology, Cairo, Egypt

Keywords 3D printing · Cone beam computed tomography · Model · Dimensional accuracy · Rapid prototyping

Purpose

Cone beam computed tomography (CBCT) is demonstrated to be an accurate method for linear and angular measurements [1]. Rapid prototyping has been widely used in surgical planning and simulation including implantology, orthognathic surgery, surgical reconstruction, preprosthetic surgery, as well as for the fabrication of maxillofacial prostheses [2]. This technology allows higher accuracy of surgical procedure and reduction of operating time. This study was carried out to evaluate the dimensional accuracy of both cone beam computed tomography and three dimensional printed models generated from cone beam computed tomography data using rapid prototyping.

Methods

Ten dummy fully edentulous models simulating atrophic mandibular human bone were used in this study. Three Titanium implants having length 16 mm and diameter 3.7 mm were placed in each model in different sites after preparation and intentional perforation of the inferior border of the mandible to facilitate placement of the digital caliper [3] on both apex and top of the implant to allow accurate and standardized measurement (Fig. 1a). Healing caps were then attached to the implants and the vertical combined length of the implant and the healing cap for each implant was recorded on the dummy model from facial aspect using the digital caliper (Fig. 1b).

Each dummy model was then radiographed using cone beam computed tomography. The image was then transferred to the workstation for secondary reconstruction and manipulation on the software.

On the corrected coronal cut, measurement recording was performed by drawing a line from the middle of the top of the healing cap till the apical end of the implant in its center (Fig. 1c).

Segmentation and thresholding were performed using in vivo 5.1 excluding the unwanted densities and the manipulated CBCT STL data was transferred to the workstation connected to the three dimensional printer to obtain the 3D model made of high performance composite material, in a time ranging from 3 to 4 h, then using the same digital caliper, the same measurements from the previously selected reference points were recorded on the 3D printed model generated from cone beam computed tomography data (Fig. 1d).

Measurements obtained from cone beam computed tomography were compared to the physical measurements on both the dummy mandibular models (considered as the gold standard) and the 3D printed models (see Fig. 2).

All the results were subjected to statistical analysis.

Results

The mean and standard deviation values of implant length were 22.83 ± 1.84 mm, 22.70 ± 1.93 mm and 22.74 ± 1.69 mm as measured by dummy models, cone beam computed tomography and 3D printed models, respectively (see Table 1).

There was no statistically significant difference between measurements on Dummy models and cone beam computed tomography, the later showed shorter implant length than Dummy models (Mean difference = 0.13).

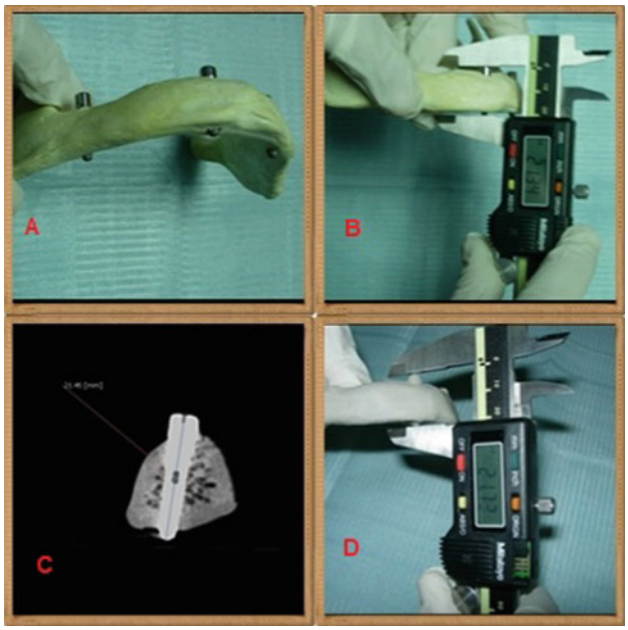

Fig. 1 **a** The initial model with implants and healing caps in place. **b** Measurement using the digital caliper. **c** Measurement on the cone beam computed tomography image. **d** Measurement on the final model generated from 3D printing

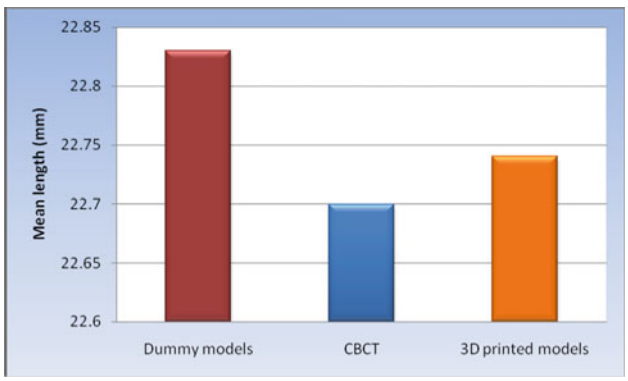

Fig. 2 *Bar chart* representing mean implant length measured by the three modalities

Table 1 Mean and standard deviation (SD) values of implant length measured by the three modalities

Modality	Mean	SD
Dummy models	22.83	1.84
CBCT	22.70	1.93
3D printed models	22.74	1.69

There was no statistically significant difference between measurements on Dummy models and 3D printed models. 3D printed models showed shorter implant length than Dummy models (Mean difference = 0.09).

There was no statistically significant difference between measurements on cone beam computed tomography and 3D printed models. 3D printed models showed shorter implant length than cone beam computed tomography (Mean difference = 0.04).

Conclusion

Three dimensional printing based on cone beam computed tomography data provides accurate replica of the original radiographed structures, allowing their use in different applications in the maxillofacial region. Cone beam computed tomography is a reliable tool in obtaining linear measurements

References

[1] Moreira CR, Sales MA, Lopes PM, Cavalcanti MG. Assessment of linear and angular measurements on three-dimensional cone-beam computed tomographic images Oral Surg Oral Med Oral Pathol Oral RadiolEndod. 2009 Sep;108(3):430–6.

[2] Goiato MC, Santos MR, Pesqueira AA, Moreno A, dos Santos DM, Haddad MF. Prototyping for surgical and prosthetic treatment. J Craniofac Surg. 2011 May;22(3):914–7.

[3] Al-Ekrish AA and Ekram M. A comparative study of the accuracy and reliability of multidetector computed tomography and cone beam computed tomography in the assessment of dental implant site dimensions. DentomaxillofacRadiol; 40: 67–75, 2011.

Validation of a surface to image registration method for orthognatic surgery

P. Van Leemput[1], D. Vandermeulen[2], G. Swennen[3], W. Mollemans[1], F. Schutyser[1]

[1]Nobel Biocare—Medicim N.V., Guided Surgery Center, Mechelen, Belgium

[2]K.U.Leuven, Medical Imaging Research Center, Leuven, Belgium

[3]General Hospital St.-Jan Bruges, Division of Maxillofacial Surgery, Bruges, Belgium and 3D Facial Imaging Research Group, Bruges, Belgium

Keywords Registration · Image gradient · Optimization

Purpose

In this lecture, we present our validation results for a novel surface to image registration technique that automatically positions a surface scan of the patient's teeth and gingiva at the correct position in the three dimensional image of the patient's skull. The skull image is derived from (cone beam) Computed Tomography data (CBCT or CT). The patient's dental region is scanned with a low radiation dose, a normal scan protocol and with the patient's head in a relaxed position. The teeth surface is obtained by taking a double sided impression of the dental area. This impression can be digitalized with a (CB)CT scan at a high radiation dose to obtain rich details. Using a surface rendering algorithm (like marching cubes), we derive a surface model from the volumetric image obtained from the (CB)CT data of the impression. Alternatively, a plaster cast can be poured from the impression. In the latter case, the surface model can be obtained directly from the cast using a medical or dental laser scanner.

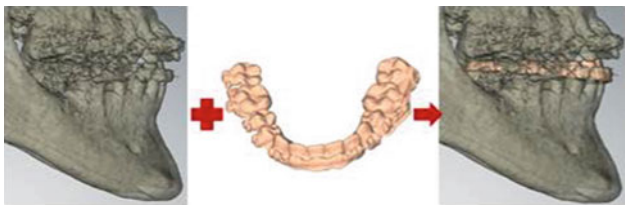

Fig. 1 The three dimensional image of the patient's skull (*left*) and the surface scan of the crowns (*middle*) are fused together in one image (*right*). The combined result can be used to set the ideal occlusion for maxillofacial surgery

We use our method in the context of orthognatic surgery, where an accurate delineation of the teeth surface is needed to set the patient's ideal occlusion during planning. Such a detailed description is provided by the surface scan but cannot be derived directly from the (CB)CT data. Hence, a fusion of both data sources is in order (see Fig. 1).

Methods

It is well known that the grey value intensity in a (CB)CT scan is proportional to the density of the scanned object. Typically, the edges of the object are marked by large image gradients, i.e. significant changes in grey value intensity when compared to the object's surroundings. Since the visible teeth surface (the crowns) corresponds to dense teeth enamel surrounded by air or soft tissue, it will generate large gradients at the teeth edges in the (CB)CT image. Ultimately, these large gradients are the target location for the surface scan of the teeth arc. Our registration method optimizes one or more gradient-based cost functions to move the surface to its correct position in image space. For practical usage, the registration methodology has been implemented in the NobelClinician software developed by Nobel Biocare.

Results

To validate our newly developed surface to image registration method, we compare the surface position obtained with our method to the surface position obtained with the triple scan procedure introduced by Swennen et al. [1]. Three dimensional distances between both results were calculated in all surface points for 35 dentate patients. The mean population distance lies between 0.3 and 0.4 mm with 95 % confidence. The voxel size of the image is 0.4 mm in all cases.

Conclusion

The validation results showed that the accuracy of our surface to image registration method is acceptable. With 95 % confidence, we obtained a mean population error smaller than one voxel, using the triple scan procedure as a reference solution. The observed accuracy is comparable to the accuracy reported in studies of other surface to image and image to image registration methods [2, 3, 4, 5]. Other registration methods, e.g. [2, 5], use fiducial reference markers added to the dental impression, dental plaster cast or patient in their scanning procedure. Using point-based rigid registration (with e.g. the Iterative Closest Point algorithm), they align the surface and CT scans of these foreign markers. Adding markers to the dental area can cause a distortion of the soft tissues. Also, these methods can suffer from a misalignment of the markers. The triple scan procedure developed by Swennen et al. [1] does not use fiducial markers but is time consuming. It requires the patient to undergo two radiation doses, one of them with an impression positioned in the mouth. Our registration method has several advantages over existing methods. First of all, the patient is only scanned once. Also, our methodology does not need

much user interaction and is minimally invasive for the patient. More specifically, no foreign objects are placed in the mouth during scanning.

References

[1] Swennen G. R. J., Mollemans W., De Clercq C., Abeloos J., Lamoral P., Lippens F., Neyt N., Casselman J., Schutyser F. (2009) A cone-beam computed tomography triple scan procedure to obtain a three-dimensional augmented virtual skull model appropriate for orthognathic surgery planning. Journal of Craniofacial Surgery 20(2): 297–307.

[2] Gateno J., Teichgraeber J. F. (2003) A new technique for the creation of a computerized composite skull model. Journal of Oral and Maxillafacial Surgery 61: 222–227.

[3] Nkenke E., Zachow S., Benz M., Maier T., Veit K., Kramer M., Benz S., Hausler G., Neukam F. W., Lell M. (2004) Fusion of computed tomography data and optical 3D images of the dentition for streak artefact correction in the simulation of orthognathic surgery. Dentomaxillofacial Radiology 33: 226–232.

[4] Noh H., Nabha W., Cho J.-H., Hwang H.-S. (2011) Registration accuracy in the integration of laser-scanned dental images into maxillofacial cone-beam computed tomography images. Americal Journal of Orthodontics and Dentofacial Orthopedics 140(4): 585–591.

[5] Uechi J., Okayama M., Shibata T., Muguruma T., Hayashi K., Endo K., Mizoguchi I. (2006) A novel method for the 3-dimensional simulation of orthognathic surgery by using a multimodal image-fusion technique. American Journal of Orthodontics and Dentofacial Orthopedics 130: 786–798.

Facilities of measurement of orbital volume using cone beam computed tomography

A. Dobai[1], T. Vízkelety[1], Z. Markella[3], O. Lukats[2], E. Maka[2], M. Kiss[4], P. Bujtár[5], A. Szűcs[1], L. Pataky[1], J. Barabás[1]

[1]Department of Oral and Maxillofacial Surgery and Dentistry, Faculty of Dentistry, Semmelweis University, Budapest, Hungary

[2]Department of Opthalmology, Faculty of Medicine, Semmelweis University, Budapest, Hungary

[3]Kálmán Kandó Faculty of Electrical Engineering, Óbuda University, Budapest, Hungary

[4]Dunaújváros College, Dunaújváros, Hungary

[5]Department of Oral and Maxillofacial Surgery, University Hospitals of Leicester, Leicester, United Kingdom

Keywords Cone beam computed tomography · Cranioviewer · Orbital volume · Enucleation

Purpose

The orbits are conical or four-sided pyramidal cavities which consist of a base, an apex and four walls. The following four borders form the base which opens in the face: (1) superior margin: frontal bone, (2) inferior margin: maxilla and zygomatic, (3) medial margin: frontal, lacrimal and maxilla, (4) lateral margin: zygomaticand frontal. The apex is found near the medial end of superior orbital fissure and contains the optic canal. Because of the complicated anatomical structure of the bony orbit such as irregular inner border, holes and fissures the measurement of its volume is difficult. The aim of this study was to create and test a method for the measurement of orbital volume by means of cone beam computed tomography (CBCT) and Cranioviewer program software (developed by Vizkelety and Markella) in case of patients who have undergone enucleation and orbital implantation and to establish whether there are any determinable differences between the volumes of the healthy and the operated orbits or between those of the healthy left and right orbits.

Methods

The basic problem about the measurement of orbital volume is that the anatomical borders of orbit can hardly be detected. On the exclusively axial or sagittal scans the most anterior and the most posterior borders are not accurately determinable. Therefore in this study the anterior borders of orbits were adjusted on axial CBCT scans and orbital volumes were measured on frontal ones by means of Craniowiever software. A large-volume CBCT scanner (iCat Classic, Xoran Technologies, Ann Arber, Michigan, USA) was used, with the following parameters: 120 kV, pixel size 0.3 mm, slice increment 0.3, and FOV height 6 cm. CBCT scans were made in 50 cases and the position of the head was close to the Frankfurti horizontal and to the sagittal midline, 10 of which were later excluded because of various technical problems. The study group therefore consisted of 20 patients (8 men and 12 women; mean age 43, 85) who had been operated on enucleation and orbital implantation. FCI synthetic hydroxyapatite had been used as the orbital implant for volume replacement in 12 cases, and aluminium (Bioceramic) in 8 cases. In 18 cases the implantation had been primary, and in 2 cases secondary. The diameter of the implant was 20 mm in 12 cases, and 18 mm in 8 cases.The longest follow-up time was 7 years, and the shortest was 1 year. The control group were made in 20 patients with various dental problems. CBCT scans were recorded for the facial region of the skull, containing the orbital region. In all 40 cases the anterior border of orbit was marked on axial scans. We marked the most dorsal points of the left and right orbit entry and frame straight lines into the two points which at the same time are the levels of the most ventral points of the orbit constitute a closed circle. The orbital frame can be denoted by red and blue lines in axial and coronal scans (Fig. 1).Then five slices were made in the ventrodorsal direction at 4.8 mm intervals in the frontal plane in both bony orbits (containing the orbital implant and the healthy one) with Cranioviewer orbital program software (Fig. 2). The Cranioviewer program can colour the area of the slices red, and it automatically measures the area in mm^2 (Fig. 3).

Results

In 5 of the 20 cases of the study group, the first 4 or all 5 slices revealed that the volume of the operated orbit was significantly smaller than that of the healthy orbit, in 12 cases only from 1 to 3 of the slices indicated such a significant difference, and in 3 cases no differences were observed between the orbits. In the control group there was no significant difference between the two healthy orbits. The accuracy of the volume measurements was assessed statistically by means of the paired samples *t* test.

Conclusion

Multislice CT and MRI allow multiplanar imaging of both the normal and pathological anatomy. In the CT technique, the scan plane is planned from a lateral scout to be parallel to the infraorbital-meatal line approximating the orbital nerve plane. Slices 3 mm thick are

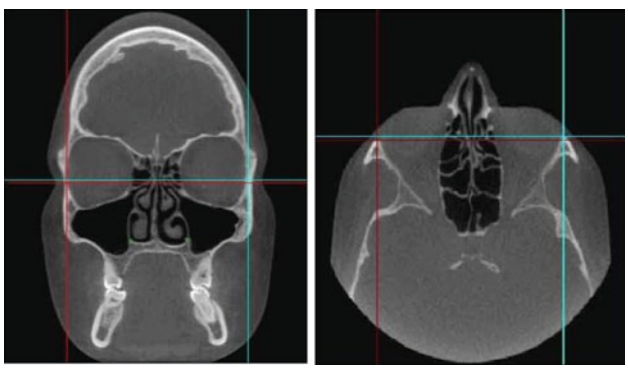

Fig. 1 The orbital frame is denoted by red and *blue lines* in coroanal and axial scan

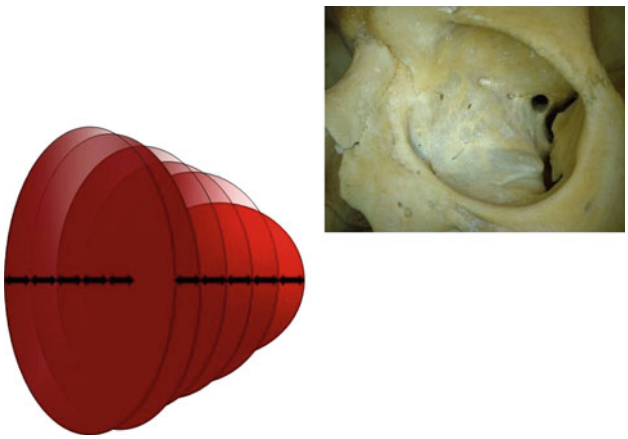

Fig. 2 Slices were made at 4.8 mm intervals in the ventrodorsal direction in the frontal plane

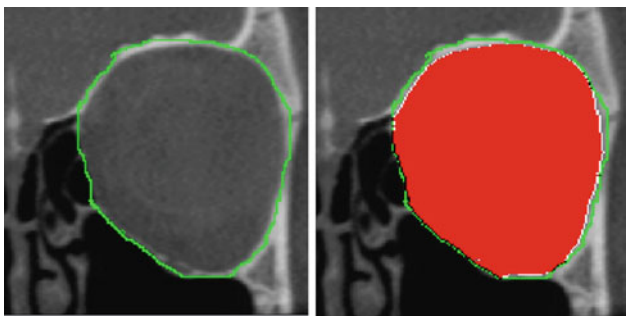

Fig. 3 The bony orbital border is marked by a *green line*, than the program automatically colours the area *red* and measures it in mm^2

preferred for routine soft tissue visualization on spiral CT because of the increased noise with thinner slices [1]. CBCT has a number of advantages comparing to conventional CT. The i-CATTM cone beam provides unprecedented imaging of the maxillofacial area with less radiation than with that of traditional fan beam CT systems [2]. In spite of all this there has been no appropriate method available for exact measurement of the bony orbital volume so far, which would be of particular importance in orbital injury reconstruction. However, the use of CBCT scans and Cranioviewer orbital program software appear to offer a reliable method for the measurement of changes in orbital volume. In our research it became evident, that the comparison of the area of the analogue frontal levels gives more accurate details of the changes in the morphology of the bony orbit than evaluating the orbits as a unified volume.

References

[1] Aviv RI, Casselman J (2005) Orbital imaging: Part 1. Normal anatomy. Clinical Radiology 60: 279–287.

[2] Olga L, Tamás V (2012) Measurement of Orbital Volume after Enucleation and Orbital Implantation. PLoS ONE 7(12): e50333.

Role of the temporomandibular joint for macroscopic biomechanics of the human mandible: a finite element study

C. Kober[1], B.-I. Berg[2], Y. Hayakawa[3], A. Gurin[4], C. Hellmich[5], V. Komlev[4,6], R. Sader[7]

[1]HAW Hamburg, Faculty of Life Sciences, Hamburg, Germany

[2]University Hospital Basel, Basel, Switzerland

[3]Kitami Institute of Technology, Kitami, Japan

[4]BioNova LLS, Moscow, Russia

[5]TU Vienna, Vienna, Austria

[6]A.A. Baikov Institute of Metallurgy and Material Science, Moscow, Russia

[7]University of Frankfurt, Frankfurt, Germany

Keywords Temporomandibular joint · Human mandible · Finite element simulation · Biomechanics · 3D modeling

Purpose

Based on the mechanical adaptation of bone, finite element simulation of mammalian skeletal organs valuably contributes to a better understanding of pathologies in this field. Nevertheless, there are still plenty of open questions subject to ongoing research, e.g. the realization of joints.

Inter alia due to its 6° of freedom, the temporomandibular joint (TMJ) is one of the most complex joints within the human body. Notably, about 20 % of the population suffer from often painful and long lasting temporomandibular disorders (TMD). Within this context, the question arises how the condition of the TMJ influences the human jaw and, one step further, how this influence is altered for the case of (1) various TMD and (2) mandibular pathologies as partial loss of dentition or atrophy. Therefore, within a detailed research project about mandibular biomechanics, the influence of the TMJ on the load carrying behavior of the human mandible has been considered.

The objectives of this contribution are, firstly, a modeling strategy for the realization of the TMJ within mandibular finite element analysis (FEA) and secondly, a sensitivity analysis concerning this strategy with special regard to pathological cases.

Methods

The highly differentiated anatomy of the TMJ consists of the joint capsule with the articular disc, several ligaments, and the retrocondylar tissue between the mandibular condyle and the temporomandibular fossa (Fig. 1, left). For mandibular FEA, the mechanical guidance by the TMJ is a boundary condition which means that its influence on the mandible is exerted via the contact surface. Thereby, the complicated inner formation of the TMJ—notably highly anisotropic and nonlinear—is only of indirect relevance.

Biomechanical simulation of skeletal organs is often based on computer tomography (CT) with reduced soft tissue contrast. Therefore, the modeling strategy is structured in two parts, (1) a refined derivation based on individual reconstruction, and (2) a generalization applicable to routine simulation.

For part I, we referred to CT data with acceptable soft tissue contrast and resolution. After application of special image processing, visualization of the TMJ capsule by direct volume rendering was possible for anatomical orientation. Thereon based, the joint capsule, the lateral ligament, and the lateral pterygoid muscle could be segmented and reconstructed in 3D (Fig. 1, middle). Inter alia with regard to the special attachment of the lateral pterygoid muscle to the articular capsule and disc, this model is by far too complex to be directly transferred to FEA of the entire mandible. Therefore, the capsule was simplified mimicking its original coverage of the

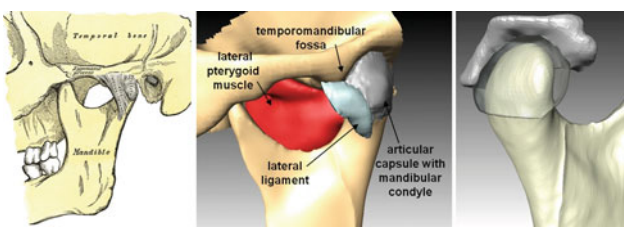

Fig. 1 Anatomy of the TMJ (*left*), refined 3D-model (*middle*), simplified capsule with part of the skull (*right*)

condyle, but without ligaments, disc, and the special attachment to the lateral pterygoid muscle. As the role of the TMJ within mandibular FEA is a boundary condition, stress and strain within the capsule are not subject of this study. Therefore, the simplified capsule was modeled as isotropic and linear with some substitute Young's modulus and Poisson ratio. The capsule's attachment to the skull was modeled by (partial) rigid attachment. The mandibular condyle and the capsule were in direct bond whereby the condyle was somehow freely mobile within the capsule mimicking the six degrees of freedom (Fig. 1, right).

For standard simulation, this individual strategy was generalized especially for reduction of modeling efforts (part II). After segmentation of the mandible, this segmentation was enlarged by about 5–7 pixels (with the mandibular segmentation locked) and cut so that only the condylar head was covered. After freeing the frontal part of the condyle for the attachment of the lateral pterygoid muscle, the additional segmentation was smoothed and reconstructed in 3D. The result is equivalent to the one of the individual strategy.

The simplified capsule could be successfully added to mandibular FEA. The modeling strategy was subjected to a sensitivity analysis with regard to (a) the capsule's shape, (b) its attachment to the skull, (c) capsular Young's Modulus, and (d) Poisson ratio. Based on micromechanical considerations, we chose the volumetric strain as indicator variable. We tested physiological biting on selected teeth with focus on pathological cases with beginning atrophy, so kind of "symmetric" case, partially edentulous and atrophic at both sides, and an "asymmetric" one with severe atrophy at one side and some residual dentition at the other one.

Results

The strategy could be successfully implemented with acceptable efforts. The sensitivity analysis revealed that a too "small" capsule, so not covering the full condylar head, produces high unphysiological strain at the condyles. A "too small" or "too large" attachment of the capsule to the skull, highly exceeding or undergoing the anatomical reality, also results in unrealistic strain profiles. The choice of capsular elastic variables showed very high quantitative influence (Fig. 2). The high compressive strain at the alveolar corpus, which we found as typical for atrophic mandibles, decreased monotonically, but non-linearly with increasing capsular Young's modulus. The same is true for increasing Poisson ratio. Interestingly, the effect on physiological loading at the mandibular incisura and ramus was non-monotonic. We found some "optimal" capsular Young's modulus of about 5 MPa where the strain profile best resembled physiological loading known from previous studies. The FEA of the case characterized by asymmetric pathology revealed that even partial dentition seemed to protect the mandible from unphysiological loading.

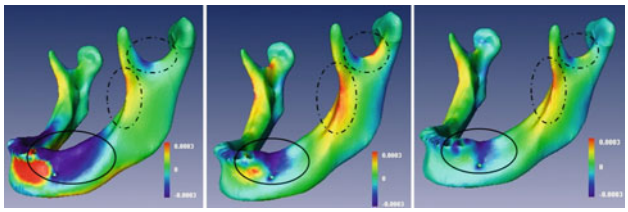

Fig. 2 Volumetric strain due to a lateral bite, capsular Young's modulus 0.1 MPa (left), 5 MPa (*middle*), and 50 MPa (*right*), *bold circles* indicate monotonically decreasing unphysiological compressive strain, *dashed circl*es indicate non-monotonic physiological loading

Conclusion

A modeling strategy for realization of the TMJ within mandibular FEA was presented and tested by a sensitivity analysis. The observed high influence of the TMJ is in agreement with clinical observations that alterations of the TMJ affect the entire jaw. The endorsement of this inter-dependence by the presence of mandibular pathologies as atrophy of the alveolar corpus, see the high unphysiological compressive strain there, indicates a vise versa stimulating procedure, whereas, on the other hand, even partial dentition contributes to protection of the mandible from unphysiological loading.

Acknowledgement

This work was supported under the Theme FP7-2008-SME-1 of the 7th Framework Programme of the Euro-pean Commission, Grant no. 232164, BIO-CT-EXPLOIT.